

# Break-up spots: Could the Pacific open as a consequence of plate kinematics?

Valérie Clouard<sup>a,\*</sup>, Muriel Gerbault<sup>b</sup>

<sup>a</sup> *Departamento de Geofísica, Facultad de Ciencias Físicas y Matemáticas, Univ. de Chile, Blanco Encalada 2002, casilla 2777, Santiago, Chile*

<sup>b</sup> *IRD, Departamento de Geología, Facultad de Ciencias Físicas y Matemáticas, Univ. de Chile, Plaza Ercilla 803, Casilla 13518 correo 21 Santiago, Chile*

Received 22 December 2006; received in revised form 3 October 2007; accepted 3 October 2007

Available online 16 October 2007

Edited by: C.P. Jaupart

---

## Abstract

The South Central Pacific is the location of an abnormal concentration of intraplate volcanism. Noting that this volcanism is present from the Kermadec Tonga trench to the Easter microplate and forms a wide east–west channel, we propose to explain its occurrence in relation to the Pacific plate geometry and kinematics. We construct 2D numerical models of stress and strain within the Pacific plate using its velocity field and boundary conditions. The models indicate a shear band, associated to a change from compressional stresses to the south to tensional stresses to the north, which develop after 10 Myr between the Australian plate corner and the Easter microplate. We propose that the Central Pacific intraplate volcanism is related to this process, and may represent the first step of a future plate re-organization which will eventually break the Pacific plate in a southern and a northern plate due to intraplate stresses. Present-day intraplate volcanism would define break up spots of the future border.

© 2007 Elsevier B.V. All rights reserved.

*Keywords:* intraplate volcanism; Pacific; weakness zone; lithospheric stress; plate boundary

---

## 1. Introduction

Earth volcanism is attributed to 3 phenomena: mid-oceanic ridge volcanism, arc or subduction volcanism and intraplate volcanism associated to hotspots. However, hotspot volcanism does not fit well into the plate tectonic theory associated with mantle convection (Richards et al., 2000). Initially, hotspot volcanism was attributed to deep mantle plumes created in the lower mantle (Morgan, 1972). In the classic hotspot theory, plumes ascend from the Core–Mantle Boundary (CMB)

through the mantle, and develop a head responsible for Continental Flood Basalts (CFB) when reaching the surface. The subsequent tail is responsible for hotspot intraplate volcanism (Richards et al., 1989). However, hotspots have sparse geodynamical, geochemical or temporal characteristics, and multiple classifications rapidly appeared. The first classification, at the beginning of plate tectonics theory, related some hotspots to spreading ridges. Morgan (1971) argued that spreading ridges correspond to weak zones opening the lithosphere as a consequence of traction from their edges, while Wilson (1973) proposed that mid-oceanic ridges may form where several strong hotspots are able to break up the lithosphere. This hypothesis was revisited by Sheth

---

\* Corresponding author. Tel.: +56 2 978 42 96; fax: +56 2 696 86 86.  
E-mail address: [valerie@dgf.uchile.cl](mailto:valerie@dgf.uchile.cl) (V. Clouard).

(1999), who showed that flood basalt events, like Deccan and Siberian Traps or East Greenland CFBs, occurred a few tens of Myr after progressive tensional conditioning of the lithosphere and was followed by splitting along pre-existing lithospheric discontinuities. In the case of the opening of the Atlantic, continental rifting was active for 25 Myr before and 25 Myr after the main magmatic event (McHone, 2000). The most recent classification (Courtilot et al., 2003) attempted to relate the 49 most cited hotspots to three different sources, following 5 criteria: long-lived tracks, traps at their initiation, topographic swell, specific  $^4\text{He}/^3\text{He}$  or  $^{21}\text{Ne}/^{22}\text{Ne}$  ratios, and low shear velocities ( $V_s$ ) at 500 km. Courtilot et al. (2003) divided the studied hotspots into those originating in the lowermost mantle, which would be 7 including the Hawaii, Louisville and Easter–Crough hotspots in the Pacific, those that would originate from the transition zone above a superplume (Davaille, 1999), among which

they counted the Central Pacific hotspots, and those that would be linked to intraplate stresses within the lithosphere (Anderson, 1998). Thus, intraplate stresses could possibly generate intraplate volcanism. However, the only effective evidence for intraplate volcanism related to tensional stresses came recently from young volcanoes offshore Japan, associated to plate flexure prior to subduction (Hirano et al., 2006). These authors proposed a source in the upper asthenosphere, similar to that of Mid-Oceanic-Ridge Basalts (MORB).

In this study, we propose to explain the origin of the central Pacific hotspots in relation to stresses within the Pacific Plate, due to its particular geometry and kinematics. We start from the observation that from the Kermadec Tonga trench to the Easter microplate (Fig. 1), a group of recent and presumed non-deep Pacific hotspots (Clouard and Bonneville, 2001; Courtilot et al., 2003) exist, and hypothesize that this is not a coincidence. Using

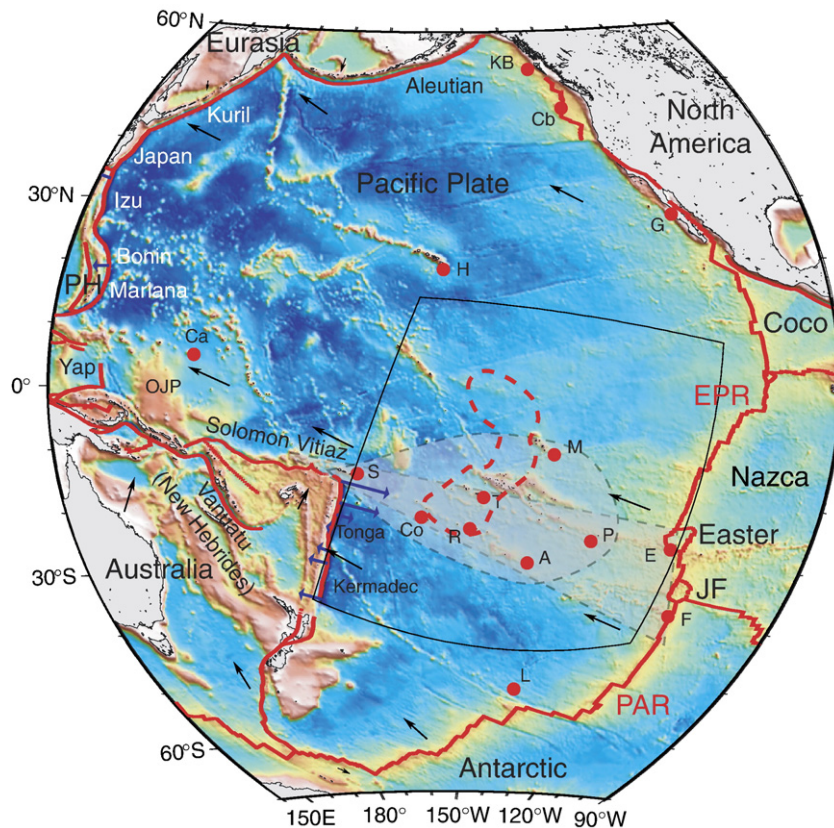


Fig. 1. Bathymetry of the Pacific and neighboring plates. Name of plates in bold (PH stands for Philippines and JF for Juan Fernandez). Name of subduction zones in black or white and of mid-oceanic ridges in red. Black thin arrows: Euler vectors from NUVEL-1A-NNR (original scale 1 cm=7 cm/yr). Blue arrows: Trench absolute velocities. Red dots: Pacific hotspots (H: Hawaii, Ca: Caroline, S: Samoa, Co: Cook, R: Rurutu, A: Austral (McDonald), T: Tahiti, M: Marquesas, P: Pitcairn, E: Easter–Crough, F: Foundation; G: Guadalupe; L: Louisville; CB: Cobb; KB: Kodiak Bowie). OJP stands for Ontong-Java Plateau. Red lines: plate boundaries. The limit of the 400-m abnormal elevation of the Superswell is the red dashed line. The black dashed lines underline 2 possible grouping of the Pacific hotspots. The black frame is the model domain.

the observation of Wilson (1973) and Morgan (1978) linking mid-oceanic ridges and hotspots, this alignment could also forecast a region of future reorganization of plate boundaries. Plate motions evolve over various time scales (Bercovici et al., 2000). Convective type plate driving forces can only evolve at convective time scales ( $\geq 100$  Myr). However, some changes in plate motion are too rapid to be caused by convection (Lithgow-Bertelloni and Richards, 1998) and are attributed to superficial phenomena like the annihilation of a subduction boundary by continental collision, the disappearance of a ridge by subduction or the initiation of a new subduction zone (Bercovici et al., 2000). If we look at the Pacific history, the last main change that occurred is the interruption of subduction to the north of the Australian plate at 5–7 Ma (Hamburger and Isacks, 1987). This change indicates a modification in external forces acting on the Pacific plate with respect to the Australian plate. Consequently, the Pacific plate might tear, and intraplate volcanism would be the result of transtensive stresses in the upper mantle and in the lithosphere.

To illustrate this large plate-scale process, we develop plane strain numerical models of an area corresponding to the Pacific plate from the mid-oceanic ridge to the subduction zone under the Australian plate, with differential velocities applied on the northern and southern part of the plate because of absolute trench motions. Our aim is to demonstrate that the kinematics and geometry of plates at the large scale play a key role in their evolution through time. Four numerical models test the possible influence of boundary conditions. Finally, we present a synthesis of evidence that lead us to conclude that the central Pacific intraplate alignment should be the location of a future break up of the Pacific plate and that this anomalous volcanism defines break up spots instead of pure hotspots.

## 2. Tectonic setting

The present day geometry of the Pacific plate, the active Pacific hotspots, the tectonic context and in particular the stability of plate boundaries, ridges, subduction zones and plate motion velocities, provide the boundary conditions of our modeling analysis.

### 2.1. The Pacific plate settings

The Pacific plate is the largest of the tectonic plates. It is created at the East Pacific Rise (EPR) and Pacific–Antarctic Rise (PAR), slips along north America and subducts everywhere else. Its age reaches 180 Ma in the northwestern Pacific. The present day geometry of the

mid-Pacific ridges began to form from 84 Ma to 16 Ma (Atwater, 1989; Mayes et al., 1990) and has been stable since this time. In addition, the creation of the Juan Fernandez and Easter microplates began between  $\approx 5$  and 6 Ma and continues today (Anderson-Fontana et al., 1986; Naar and Hey, 1991).

The Pacific plate is characterized by a broad area of anomalous shallow seafloor depth named the South Pacific Superswell (McNutt and Fisher, 1987), the limits of which were recently defined (Adam and Bonneville, 2005). It extends from 10°N to 30°S between longitudes 130°W and 160°W with a semi-donut shape open to the west (Fig. 1). Geoid values associated with the Superswell area show that its northern branch can be correlated with a density anomaly at about 300 km depth (Adam and Bonneville, 2005), whereas a dynamic explanation remains to be found for the southern branch (McNutt and Fisher, 1987; Adam and Bonneville, 2005), which is superimposed on the hotspot alignment.

The present-day active Pacific hotspots are plotted on Fig. 1. Cobb, Bowie and Guadalupe are excluded of our analysis as they are far to the north of our study area. Tomographic images obtained from S-wave velocities show a deep plume beneath the Cook, Samoa, Tahiti, Easter, Louisville and Hawaii hotspots (Montelli et al., 2006). However, using more restrictive criteria, only Hawaii, Easter and Louisville have been classified as resulting from a primary deep plume (Courtillot et al., 2003). The 9 other hotspots, Caroline, Samoa, Cook, Rurutu, Tahiti, Macdonald, Marquesas, Pitcairn and Foundation do not present the characteristics of deep plumes (Clouard and Bonneville, 2001; Courtillot et al., 2003) and are all active since 7 Myr or less (Clouard and Bonneville, 2005). Apart from these active volcanoes, the South Central Pacific seafloor is marked by older volcanism, such as the Tuamotu Islands around 40 Ma (Ito et al., 1995) or the Austral–Cook region, which is characterized by successive intraplate events from 54 Ma to present (Clouard and Bonneville, 2005). Geochemical variability indicates that recent hotspot volcanism in the Austral–Cook region is clearly separated from older volcanism (Bonneville et al., 2006). The same South Central Pacific region was also responsible for the Cretaceous intraplate volcanism now located in the northwest Pacific. No simple reconstruction can relate this old volcanism with the present-day hotspots (Clouard and Bonneville, 2001; Koppers et al., 2003). To explain both recent and old volcanism, the hypothesis of a superplume below the Superswell area has been proposed (McNutt, 1998). Davaille (1999) constructed an analogical model of a superplume that would oscillate between the CMB and

the surface with a 100 m.y. recurrent time. In that case, a huge, hot and chemically heterogeneous instability born at the CMB exists in the mantle and hotspots rise from its top to the surface. Tomographic images provide evidence of such an anomaly (e.g., Grand et al., 1997), which does not reach the surface because of the transient and oscillating nature of the upwelling phenomena (Davaille et al., 2005).

The term “Central Pacific hotspots” usually refers to hotspots geographically associated to Polynesia or the Superswell areas. In our analysis, we include all the active hotspots from the Kermadec Tonga trench to the EPR. Fig. 1 shows that they are distributed almost regularly between the Samoa hotspot (westernmost) and the Easter hotspot (easternmost). They can be described as forming a 10° width fan, initiating from the north Australian corner and ending at the Easter and Foundation hotspots, or a horizontal drop, initiating from the same place and bordered by the Marquesas, Pitcairn and Austral–Macdonald hotspots.

## 2.2. Pacific plate boundaries

Our model domain corresponds to an 5500 km width square box that comprises a part of the Pacific plate extending eastward from the EPR, to the Kermadec Tonga trench westward (Fig. 1). Top and bottom model horizontal borders correspond to what we will name southern and northern borders, and left and right limits correspond to western and eastern borders. We choose the horizontal borders to be within the Pacific plate, oriented parallel to the Pacific plate absolute motion (towards negative  $X$  direction). They are subjected to forces internal to the Pacific plate, rising from further away active external forces due to subducting and rifting boundaries. Appropriate boundary conditions are thus likely to be either completely free, or free-slip (horizontal movement parallel to plate absolute motion), which effect will be tested with the models. The eastern limit of our box corresponds to the mid-Pacific ridge. This spreading boundary has been quite stable since 16 Ma, except for the creation of the microplates of Easter and Juan Fernandez, which mark the transition between the EPR and the PAR. The northwestern boundary of our box remains far away from its subduction zones to the north–west, quite stable over the last 20 Myr (Heuret and Lallemand, 2005). Therefore we can approximate details of the various subduction zones along the Kuril, Japan, Izu-Bonin, Mariana and Yap trenches with a unique boundary condition.

To the south–west, the limit of our box is in front of the Australian plate subduction, which existed at least

since about 50 Ma (Gill and Gorton, 1973). However, the nature of its northern contact with the Pacific plate changed during the last millions of years. Subduction of the Pacific plate occurred along the Solomon–Vitiav trench system until about 5–7 Ma, after which the trench jumped across the Vanuatu island arc, initiating subduction of the Australian plate at the New Hebrides trench (Hamburger and Isacks, 1987). This jump was interpreted as resulting from a slab avalanche that would have occurred at 8 Ma (Pysklywec et al., 2003). A tomographic model (van der Hilst et al., 1997) shows that the Pacific slab teared at the corner between the Kermadec Trench and the former Solomon–Vitiav trench. We think that this tearing triggers asymmetric distribution of slab pull forces to act on the western edges of the Pacific plate. Additionally, from an alignment of seismic data north of the Australian plate and bathymetric data of the Pacific plate that present the shape of a fore-arc, Kroenke and Walker (1986) proposed that a new subducting plate boundary is forming north of the Ontong Java Plateau, linking the Tonga Trench and the Mariana Trenches.

We will assume that new boundary conditions acting on the Pacific plate domain initiated at about 8 Ma, when the northern boundary between the Australia and Pacific plates began to reorganize. At that time, the “initially” homogeneous westward drift of the Pacific plate started to split into a northern and a southern segment. To represent this boundary condition in the model, we apply a differential velocity between the northern and the southern segments of its western boundary.

## 2.3. Plate velocities

The motion of the Pacific plate deduced from the NUVEL-1A model (DeMets et al., 1990, 1994) is not significantly different from GPS solutions (Beavan et al., 2002). It is about 5 to 7 cm/yr depending on the distance of the point to the rotation pole of the plate (NNR reference frame). Very sparse GPS data exist presently over this extremely large domain, and deviations from rigid plate motion are less than 1 mm/yr, which is also of the order of the measurement error (Beavan et al., 2002). Therefore we can indeed consider that the Pacific plate has an homogeneous velocity everywhere, taken at 0 cm/yr in our model. However, along our western border, the trench retreats at Tonga, related to back-arc opening and Australian plate motion (Pelletier et al., 1998). Trench retreat decreases southward from about 9 to 4 cm/yr between 15°S and 21°S, and the trench is stationary at 23°S (Heuret and Lallemand, 2005). Analogical models and a compilation

of 160 trench/plate velocities evidence a linear correlation between the plate motion normal to the trench and the trench motion (Faccenna et al., 2007). Advancing trench (motion towards the volcanic arc, which is the case of the northwestern Pacific trenches) promotes faster plate velocities and retreating trench (as at the Tonga trench) slower motions. According to this empirical law, the southern segment of our box might have a motion slower than the northern one. Adopting the coefficient of 0.93 relating the trench/plate velocity (Faccenna et al., 2007), with an westward advancing trench velocity of about 4 cm/yr in front of the Mariana trench and an eastward retreating velocity between 8 and 0 cm/yr in front of the Tonga trench, the south Central Pacific plate might be 3 to 11 cm/yr slower respectively than the north. Obviously, this is not the case because of the non-linearity of velocity transfer across the subduction channel into the rigid Pacific plate, and the Pacific plate velocity in front of the Tonga trench is one of the 3 exceptions to the empirical law proposed by Faccenna et al. (2007). However, we think that the trench retreat at the Tonga trench tends to slow down the South Pacific velocity and we assume that it can be represented in our numerical models by a moderate value of 1 cm/yr. Adapted to the boundary conditions of our model, this relative change in traction (or velocity) is equivalent to block the southern segment and to impose a traction (or velocity) on the northern segment of 1 cm/yr. Timing of deformation is proportional to the applied velocity: for example a difference from 1 cm/yr to 2 mm/yr, in westward traction between the North and the South Pacific, multiplies by 5 the time necessary to develop internal deformation throughout the Pacific plate.

### 3. Plate tectonics: from rigid blocks motion to internal deformation

The theory of plate tectonics assumes that plate interiors behave rigidly while deformation is confined along their boundaries. The plate rigidity hypothesis finds its validity in the general agreement between the kinematic plate motion model NUVEL-1A derived from geological information (DeMets et al., 1994) and space geodetic measurements (Prawirodirdjo and Bock, 2004; Sella et al., 2002).

In agreement with this rigid property of plates, since the mid-1970s, theoretical metal plasticity (Hill, 1950; Odé, 1960; Kachanov, 1974) was successfully applied to large-scale tectonics, showing that lithospheric scale faults may form and create new plate boundaries, as a consequence of plate kinematics (Tapponnier and Molnar, 1976; Regenauer-Lieb, 1999; Provost et al.,

2003). Rigid plasticity provides the geometry of slip-lines or faults that bound rigid blocks, together with a stress distribution that satisfies a limiting yield stress and a velocity field. It was also shown that a small amount of dilatation along shear bands (slip-lines) cutting through the lithosphere, may open pathways for magmatic fluids, and thus transfer melts and gases from the upper mantle upwards to the surface (Regenauer-Lieb, 1999).

Although the behavior of a lithosphere varies with depth according to its thermal and compositional properties (Brace and Kohlstedt, 1980; Kohlstedt et al., 1995), the use of plane-strain plasticity at the lithospheric scale consists in defining a single yield stress  $k$  that approximates the strength of the lithosphere vertically (Regenauer-Lieb and Petit, 1997). This vertical averaging of stress and strain is similar to approaches in which the lithosphere is a thin sheet of fluid (e.g., England and McKenzie, 1983) and appears appropriate where the horizontal dimensions of a region exceed by many times the thickness of the lithosphere. For example, a yield stress  $k=108$  MPa (Regenauer-Lieb, 1999) is used to average the integrated strength of the European plate, which in reality is composed by crust and mantle multi-layers of variable composition and thus variable strength. In contrast here for the Pacific oceanic lithosphere, the concept of vertically averaged integrated strength is even more applicable, since its strength is mostly controlled by a single mantle layer, of probably greater integrated strength than the one considered for the European continent.

In reality, tectonic plates are not rigid: systematic discrepancies between GPS site velocities and those predicted by Nuvel-1A across the Andes, the Himalayan-Tibetan plateau, or Taiwan, indicate diffuse plate-boundary deformation and significant intraplate deformation (Khazaradze and Klotz, 2003; Leffler et al., 1997; Yang and Liu, 2002). Mechanical studies also indicate internal deformation of oceanic plates. For example, the Central Indian Ocean was extensively studied, west of the Ninetyeast aseismic ridge, where high intraplate seismicity is attributed to stresses transmitted from the Indian-Asia collision (Weissel et al., 1980; Shemenda, 1992; Gerbault, 2000). There, the proposed mechanism is that under increasing compression, the oceanic lithosphere first loads elastically, then develops a stage of lithospheric scale buckling as a transition from diffuse to localized deformation, until final, future plate break-up (Shemenda, 1992; Gerbault, 2000). Internal deformation of oceanic plates is not restricted to compressional settings. For example in this same Indian plate but east of the Ninetyeast aseismic ridge, strike-slip deformation was also reported by

Deplus et al. (1998), from multiple geophysical data: along at least 1000 km, left-lateral north–south strike-slip faults reactivate fossil fracture zones.

## 4. Numerical modeling

### 4.1. Method

We employ Parovoz (Poliakov and Podladchikov, 1992), a 2D plane-strain finite-differences numerical code based on the FLAC technique (Cundall and Board, 1988). It resolves differential equations alternately, with the output of the equations of motion used as input to the constitutive equations for a progressive, time-explicit, calculation. FLAC is based on 4-node quadrilateral meshes formed by superposing two constant stress/constant strain triangular finite elements. Each element behaves according to a prescribed stress/strain constitutive law in response to the applied forces or velocity boundary conditions. Parovoz is used in various studies such as localization of shear bands and fractures (Poliakov and Podladchikov, 1992; Hobbs and Ord, 1989; Gerbault et al., 1998; Lavier et al., 1999) and lithospheric extension and collision (Burov and Poliakov, 2001; Gerbault et al., 2003).

### 4.2. Model setup

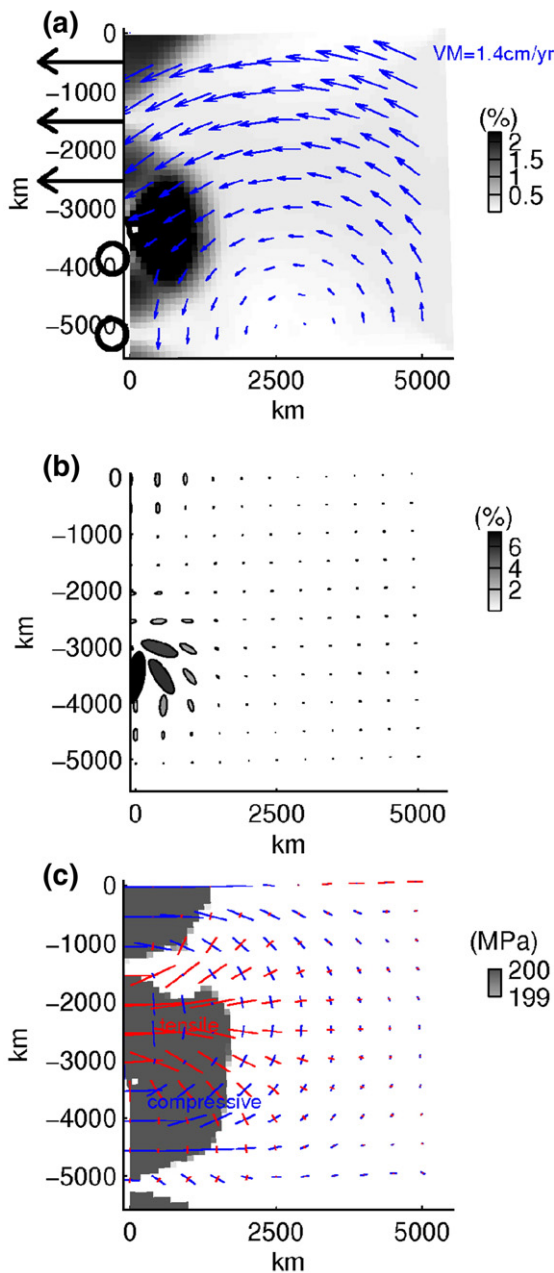
The dimensions of our domain is  $55 \times 55$  elements of size  $100 \text{ km} \times 100 \text{ km}$ , in the  $X$  and  $Y$  directions. We use elastic–brittle Mohr–Coulomb behavior in the first 3 models, and add Maxwell temperature-dependent viscoelasticity in the last model. A number of simplifying assumptions are made.

- Sphericity of the Earth: the projection of our modeled square box (Fig. 1) is not exactly a geographical square. However, it does not change the boundary conditions.
- Domain size of  $5500 \text{ km} \times 5500 \text{ km}$ : it represents about a third of the total area covered by the Pacific plate. Accounting for a larger domain make it necessary to incorporate three-dimensional subduction zones, but also to include irregular details of plate boundary geometry. We believe however that the size and position that we choose is sufficiently representative of the key aspects of the rigid versus deformable behavior of the Pacific plate, since we are far from boundary heterogeneities, and we are within the area where highest strength gradients are induced from cooling of the oceanic plate as it moves away from the EPR.
- The plane-strain assumption: it implies that plates are assumed not to deform at depth, in the third direction of the model. One major consequence is that subduction zones are not accounted for. A real subduction zone typically consists of a zone of transfer of material out of the horizontal plane into the vertical plane below. For the Australia–Pacific subduction zone that is close to the southwestern edge of our model, we suppose that the residual transfer of stress and strain, across the subduction zone and in between opposite plates, results in the relative motion of the northern part of the western edge relative to the southern part, in the models (see discussion Section 2.3).
- The averaged rheology of the lithosphere: large-scale behavior is controlled by an approximation of the vertically integrated strength of the lithosphere along its thickness (Kohlstedt et al., 1995; Regenauer-Lieb, 1999). Considering elastic–brittle behavior, we look for an average yield stress  $k$  of the oceanic lithosphere, defined from the classical Mohr–Coulomb criterion by an equivalent cohesion  $S_0 = k$  and a friction angle  $\varphi = 0$ . This averaged yield stress defines the strength of the lithosphere down to the depth of its brittle–ductile transition (around 30–50 km depth for a lithosphere of around 100 Myr old). Based on a study on the oceanic lithosphere (Gerbault, 2000), we choose  $k = 200 \text{ MPa}$ . This value will mainly affect the timing for plate loading, rather than the deformation patterns. In addition, a lithostatic stress of 600 MPa is applied, that mimics overburden load at a minimal 20 km depth. This value also controls timing for plate loading.
- Boundary conditions were discussed previously. The eastern edge corresponding to spreading ridges remains free. Supposing that trench retreat at the Tonga trench slows down the South Central Pacific, we block the westward motion of the southwestern edge, and impose an horizontal velocity of 1 cm/yr to the northwestern edge. In model 1, the northern and southern borders are set free.
- Timing: the model should cover a period initiating from the onset of the present day boundary conditions and should run for at least the time  $\Delta t$  necessary to load elastically the entire medium until failure.  $\Delta t$  can be evaluated from a simple approximation. The relation between shear stress and deformation is given by Hooke's law in 2D,  $\sigma_{xy} = 2 \times G \times \varepsilon_{xy} \times \Delta t = G/2 \times (V_x/\delta y) \times \Delta t$  ( $V_y$  is negligible), with a modulus of rigidity  $G = 2 \times 10^{10} \text{ Pa}$ , and a maximum shear stress  $\sigma_{xy} = k = 200 \text{ MPa}$ . With a dominant east–west velocity  $V_x = 10^{-2} \text{ m/yr}$  applied over a modeled width  $\delta y \approx 5.5 \times 10^6 \text{ m}$ , failure develops through the model after time  $\Delta t \approx 5.5 \text{ Myr}$ .

## 5. Results

We present here the results, after 10 Myr, of 3 models that test boundary conditions, from the simplest to the more complicated, plus one that models the effect of age on the rheology of the Pacific plate.

In model 1, (Fig. 2) the north and south borders of the model are set completely free, similarly to the eastern border. The applied westward velocity along the north-



western edge, together with the fixed southwestern edge of the model, generates counter clockwise rotation of the entire model. Cumulated Shear deformation (second invariant  $\varepsilon_{II} = \sqrt{(\varepsilon_{xx} - \varepsilon_{yy})^2/4 + \varepsilon_{xy}^2}$ , includes both elastic and plastic components) concentrates around the point of applied velocity discontinuity on the western edge of the model, adopting the typical triangle shape of corner indentation (e.g., Hill, 1950). Superimposed on areas of maximum shear strain, the shear stress (second invariant  $\sigma_{II} = \sqrt{(\sigma_{xx} - \sigma_{yy})^2/4 + \sigma_{xy}^2}$ ) reaches its yield value (200 MPa, grey zones in Fig. 2c. Principal stresses associated to this rotational deformation are compressive in the southwestern portion of the model (blue axes correspond to most compressive principal stress  $\sigma_1$ , and domains with longest axes have positive pressure in Fig. 2c), and tensile in the middle-west, where rotational traction is greatest (red axes corresponds to less compressive principal stress  $\sigma_2$ , and domains with longest axes have negative pressure).

In model 2 (Fig. 3), the north and south borders of the models are set free-slip, meaning that north–south motion is prohibited at these boundaries. Localized deformation develops from about 4 to 10 Myr from the western Australia–Pacific discontinuity boundary, propagates into the Pacific plate eastward and cuts it in two from west to east (Fig. 3a). After 10 Myr, strain ellipses within this developing shear band indicate a northwest direction of elongation of about 3.5% (Fig. 3b). A tensile state of stress develops to the north, while a compressive state of stress occurs to the south (corresponding to largest red and blue axes of principal stresses, respectively in Fig. 3c). Two spots of brittle deformation develop along the eastern edge of the modeled Pacific plate (Fig. 3a), associated to a “tearing” effect of the free vertical eastern edge (two changes in slope). These two zones may possibly be related to the recent appearance of both Easter and Juan Fernandez

Fig. 2. Model 1: Deformation and stress patterns after 10 Myr with  $V_x = 1$  cm/yr along the northern portion of the western border. a) Velocity vectors (VM gives their maximum length) superimposed on accumulated shear strain (elastic and plastic second strain invariant, see text). Boundary conditions: disks for free slip, arrows for traction. b) Ellipses of accumulated shear strain (different color scale from a). Deformation develops from the western discontinuous boundary condition, eastward into the modeled Pacific plate. c) Stress field: the second stress invariant (see text for formula) is plotted with a grey color scale, set close to the yield value ( $k=200$  MPa) in order to show zones of brittle failure. Crosses of principal stresses, where red axes correspond to least compressive  $\sigma_2$ , and blue axes correspond to most compressive  $\sigma_1$ . Largest red or largest blue axes indicate areas of either negative pressure (tensile  $P$ ) or positive pressure (compressive  $P$ ,  $P = (\sigma_1 + \sigma_2)/2$ ). Line crosses have a maximum length of 400 MPa (when the other axis is null, and where the yield stress is reached ( $k = (\sigma_2 - \sigma_1)/2$ )).

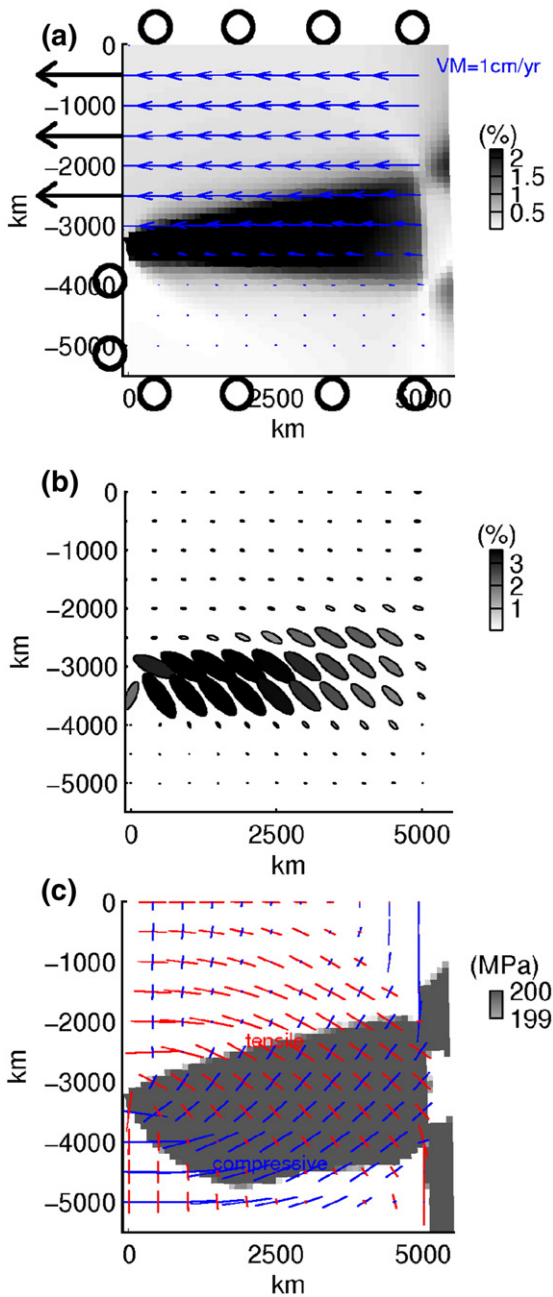


Fig. 3. Model 2: Deformation and stress patterns after 10 Myr. Same legend as Fig. 2. In addition to the model 1, the southern and northern borders are free slip, which produces a purely E–W shear zone, and separates areas of tensile stress to the north, and compressive stress to the south. Note the formation of two zones of localised deformation to the east, as shearing affects the eastern edge, corresponding to changes in slopes of the free vertical border.

microplates. This simple model presents a good correlation between its east–west shear band and the central Pacific hotspots grouped as a fan, from Samoa to the Easter and Foundation hotspots.

Model 3 (Fig. 4) tests an intermediate situation between models 1 and 2, since the northern border remains free, and the southern border is set free-slip. The system now builds a strain pattern in which the localized major E–W shear zone deviates southwestward, but also

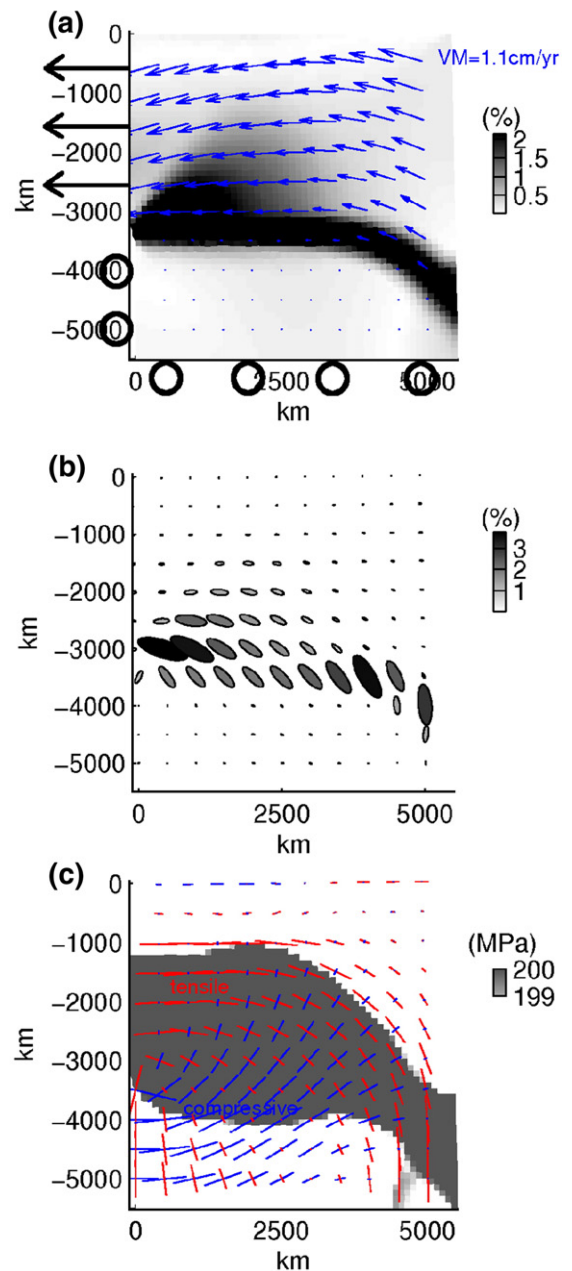


Fig. 4. Model 3: Deformation and stress patterns after 10 Myr. Same legend as Fig. 2. In addition to model 1, the southern border is free slip, which produces an E–W shear zone trending to the south at its eastern extremity. East–west compressive stresses to the south, and east–west tensile stresses to the north, rotating to north–south tensile stresses along the free eastern border.

displays a diffuse zone of deformation, in the northwest domain adjacent to the major shear zone. Additional tests show that this geometry does not depend on distance to the southern edge of the model. The stress pattern that bounds compressive from tensile stresses now displays a circumferential pattern (Fig. 4), with north–south tension along the free eastern border.

Model 4 (Fig. 5) has identical boundary conditions to model 2, but rheology is now elastic-viscous-brittle, in order to simulate east–west strength dependence on lithospheric age. This model could better approximate the response of the Pacific plate due to E–W variations

in strength. We account for a temperature averaged at 30 km depth, a depth that corresponds approximately to that at which lithospheric strength is greatest. Temperature decreases according to age following the classical *erf* solution (applied rate of 6 cm/yr), from  $T=1300\text{ }^{\circ}\text{C}$  along the eastern border, to  $T=300\text{ }^{\circ}\text{C}$  to the west (Fig. 5b). Viscosity ( $\mu_{\text{eff}}$ ) consequently increases westward according to the dislocation creep power law relating deviatoric stress and strain-rate  $\sigma=2\mu_{\text{eff}}\times\varepsilon=(\varepsilon/A)^{1/n}\times\exp^{E/nRT}$ , with parameters  $A$ ,  $n$ ,  $E$  of dry olivine (Ranalli, 1995). In the model, each element takes the minimum of the elastic-brittle and of the Maxwell

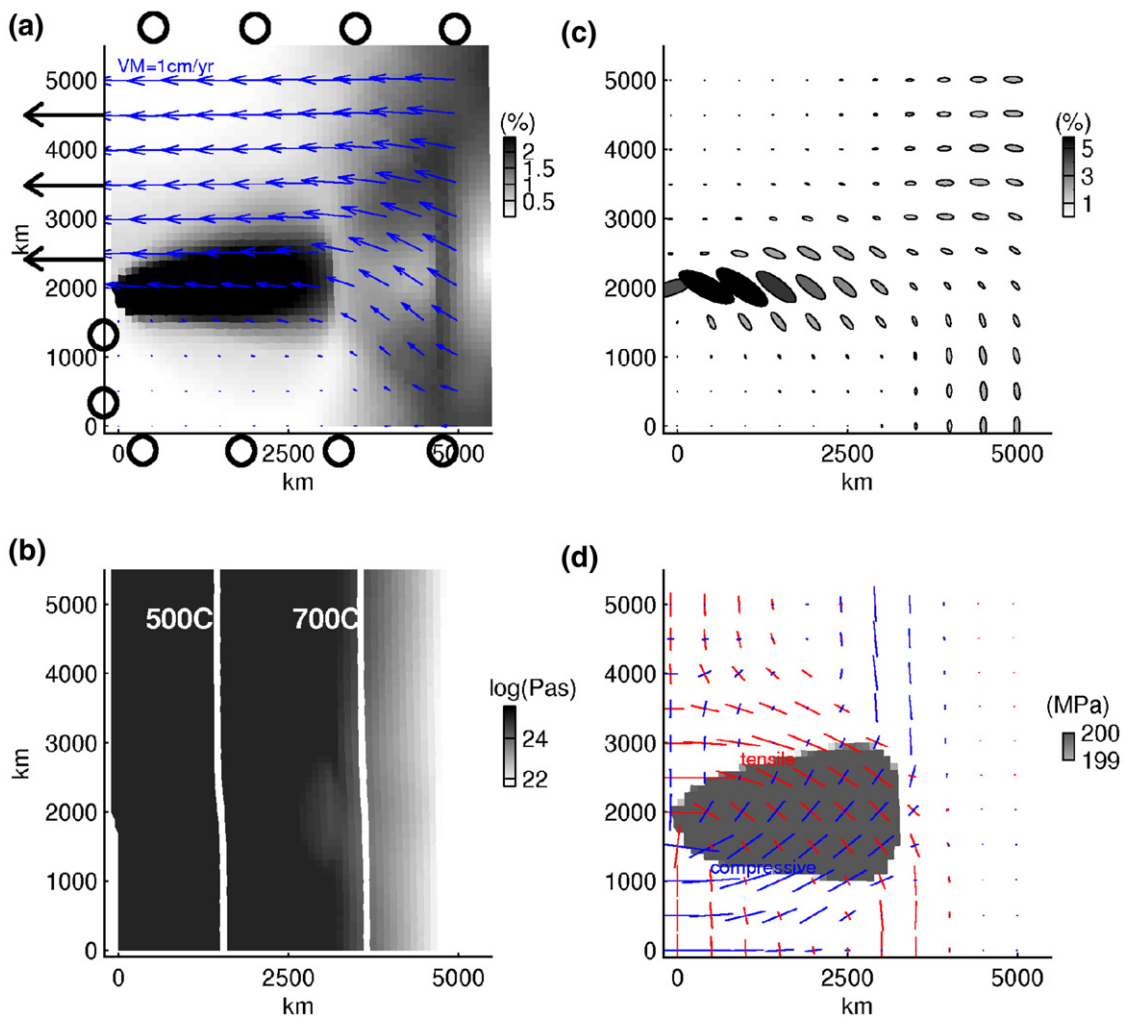


Fig. 5. Model 4: Deformation (a,c), effective viscosity (b) and stress patterns (d) after 10 Myr. In addition to boundary conditions equal to model 2, a westward decrease in temperature of the Pacific plate (two isotherms shown on b) provides a variable effective viscosity. (a,c,d) Same legend as Fig. 2. Note in (a) the non-linear switch from localised brittle deformation at about  $x=3000\text{ km}$  to fully ductile and diffuse deformation at about  $x=4800\text{ km}$ , and the formation in between of two zones of greater deformation spreading to the east, comparable to model 2. The north–south alignment of this deformation results from the geometry of the imposed temperature gradient, see (b). b)  $\log_{10}$  of the effective viscosity in Pas. Note deviated isotherms after 10 Myr of advection by westward shearing. d) Stress patterns. Note the circular brittle shear zone, compared to model 2.

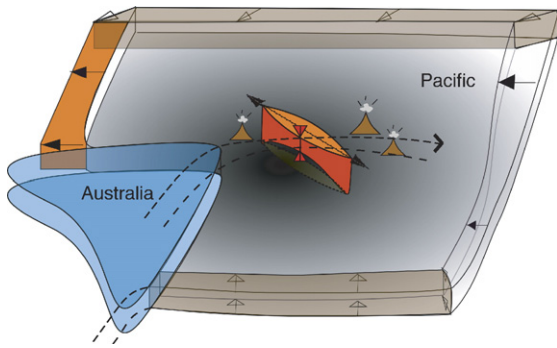


Fig. 6. Scheme of strain distribution in the Pacific lithosphere. Westward drift of the Pacific plate (in orange) is blocked to the south by the Australian indenter (in blue). Planar elongation may be associated to 5% of lithospheric thinning (in red) where intraplate volcanism can occur. The dashed line represents the subducted Pacific plate and the prolongation to the surface of the tearing, that might propagate eastward to the mid-oceanic ridge due to lithospheric-scale shear stress. (For interpretation of the references to color in this figure legend, the reader is referred to the web version of this article).

visco-elastic stress (Ranalli, 1995; Gerbault, 2000). Results after 10 Myr show that shear deformation forms an E–W shear zone inside the Pacific plate (with a maximum of about 5%) that becomes progressively more diffuse towards the east (Fig. 5a), as material becomes more ductile. The vertical patterns at about  $x=3000$  km, and about  $x=4800$  km correspond to a non-linear diffusive effect of the imposed east–west thermal gradient, as the elastic-brittle behavior switches to the power-law Maxwell behavior. This brittle-ductile transition occurs approximately where the 650 °C isotherm attains 30-km depth (Fig. 5b). In this model, the high shear stress pattern has now a circumferential shape of ‘radius’ that depends on the position of this brittle-ductile boundary (Fig. 5d). This circumferential shape is close to the position of the observed Pacific Superswell, suggesting a link between stress loading, and internal deformation in the vertical direction, e.g., thickness, of the Pacific plate (see discussion). In addition, if we compare this modeled deformation zone with the location of hotspots, it comprises all the south Central Pacific hotspots grouped as a drop (Fig. 1), and excludes Easter and Foundation.

The Pacific plate seems to have today a bivalent behavior: although it can still be considered like a rigid plate, it may also be deforming internally due to the restricting kinematics at its boundaries with the Australian plate. We propose that this internal deformation is now starting to localize in a plastic manner in the central South Pacific area (plasticity in the sense of irreversible deformation, either brittle or ductile). Internal deformation (Figs. 3c and 5c) indicates elongation in the north–

west orientation of the model, associated to north–east oriented shortening. This is partly due to the plane-strain assumption of these models. Transposed to the three-dimensional reality, this north–west oriented elongation should also affect the entire thickness of the oceanic lithosphere, not only its lateral “plane-view” dimensions (Fig. 6). It may be, that for the Pacific plate to accommodate north–east superficial elongation (in plane-view), it carries material from depth and shrinks vertically over its thickness on a localized and centered area. Therefore, one may visualize that the elongated direction of strain ellipses in plane-view models, should be accommodated vertically by thinning of the Pacific lithosphere (Fig. 6). Transposition of a maximum of 5% north–east elongation to a lithosphere 100 km thick, leads to a thinning of 5 km.

## 6. Discussion

Assuming that the Tonga–Kermadec trench retreat induces a slowing down of the westward displacement of the south Pacific plate, our numerical models indicate intraplate shearing, localized deviatoric strain and rotating deviatoric stress. They evidence an east–west trending shear band, corresponding to the location of Central Pacific volcanism. The Central Pacific lithosphere is weakened and sheared in an area corresponding to the observed hotspots. With a temperature dependent rheology, a more diffuse pattern develops, excluding the easternmost hotspots of Easter and Foundation, but more similar to the Superswell area. In this case, the Pacific intraplate volcanism would correspond to the formation of melting columns in the upper asthenosphere, in response to shearing plate boundary conditions. Central Pacific hotspots should be seen as break-up spots of shallow origin.

In the case of a pre-rifting environment, Sheth (1999) showed that CFBs are probably the product of lithospheric splitting, which permits adiabatic ascent from depths greater than plate thickness and extensive melting, and consequently establishes a high melting column. Pacific hotspots could then be the first premise of this melting generation. Intraplate ductile void growth was also proposed to explain volcanism linked with the Alpine collision, with a small amount of dilatancy along shear bands being able to transfer melts through the lithosphere (Regenauer-Lieb, 1999). This process can also be compared with the Main Ethiopian rift (Keir et al., 2006), and slow-spreading mid-ocean ridges (Escartin et al., 1999), where magma intrusions accommodate the majority of the strain. More generally, in a review paper, Tackley (2000) showed that ductile

shear localization and weakening mechanisms in the mid-lithosphere, and in particular the void-volatile weakening (Bercovici, 1998; Regenauer-Lieb, 1999), should play an important role in generating weak plate boundaries.

Similar situations in which a section of oceanic plate is submitted to asymmetric distant slab pull forces have previously been studied, provoking either lithospheric bending (e.g., Chamot-Rooke and LePichon, 1989, for the Zenisu ridge) lithospheric buckling (e.g., Gerbault, 2000, for the central Indian Ocean), or lithospheric boudinage in case of tension. In the mid-Pacific ridge area covering half of our modeled area, boudinage had indeed been suggested as a mechanism to explain short-wavelength geoid anomalies (150–300 km range, e.g., Dunbar and Sandwell, 1988). But because of the small amount of estimated north–south extension, thermal stresses due to top-down cooling of the lithosphere are presently a preferred mechanism (e.g., Sandwell and Fialko, 2004 and references therein). However, if we believe our models, that there is about 5% shear deformation (in a wider area located west of these geoid anomalies), generating tension to the north and compression to the south, then we may expect the onset of processes like lithospheric thinning or boudinage, and bending or buckling, respectively to the north and south of the domain, that may associate with melt transfer from the base of the lithosphere to the surface. These are speculations that three-dimensional modeling will have to demonstrate. In any case, the effect of these asymmetric slab-pull forces on the bathymetry should be complex. As stated previously, first to the south, the retreating trench motion, related to the north-eastward indentation by the Australian plate, induces compressive stresses through the Pacific plate, that can be accommodated by either buckling or bending of the lithosphere. Then to the north, the greater slab-pull forces induce north-eastward stretching that should be accommodated by lithospheric thinning or boudinage. Both phenomena are transient, and while active can produce an elevation of the seafloor, the first one to the south, due to lithospheric bending under compression, and the second one to the north, due to isotherms up-rising by lithospheric stretching. When comparing with the Superswell shallow seafloor and the interpretation of the geoid anomalies (Adam and Bonneville, 2005), both these effects of lithospheric bending and thinning are in good agreement with a measured geoid dip to the south, and a measured geoid high to the north, respectively. On the other hand, the presence of a superplume could also participate to the Pacific intraplate volcanism, and contribute to material being expelled up to the surface,

using the already weakened area. It is a different situation to the northwestern Pacific, where the Darwin Rise does not display any positive bathymetric anomaly (Zhong et al., 2007), and neither did it evolve towards the creation of a new plate boundary, perhaps because the kinematic conditions were not similar at Cretaceous times.

Central Pacific intraplate volcanism outlines a zone of weakness, from which a new plate boundary can form. This future boundary parallels the absolute plate motion, in good agreement with the initial direction of other new rifting, spreading and subduction boundaries (Kroenke et al., 2002). Our numerical models running over 10 Myr enable to witness the formation of a wide area of shear strain, associated to rotating shear stresses. In the models, this area presents an east–west elongation and roughly connects the northern Australian plate with the EPR. Since these plane-strain models can only generate shear zones, 3D modeling would be necessary to determine if this shear zone will evolve as a convergent, divergent or strike-slip boundary. However, evidences exist that lead us to argue for a future spreading boundary. To evolve into plate opening (characteristic time scale of the order of 50 Myr (Sheth, 1999; McHone, 2000), a divergent motion is needed between the northern and southern parts of the Pacific. Several arguments support this hypothesis; first, from plate kinematics. The asymmetric distribution of slab-pull forces acting on the Pacific plate, in front of the Australian plate and in front of the Philippine and Eurasian plate further north 5000 km away, may help to create divergence. Along the northern margin of the Australian plate, friction between the buoyant Ontong-Java plateau may trigger tensile stresses in the Central Pacific (Wessel and Kroenke, 2007), while tomographic images of the former Solomon–Vitiav trench (van der Hilst et al., 1997) indicate a tearing of the subducted Pacific plate that could propagate eastward at the surface (6). And to the east, the geometrical division of the mid-Pacific ridge into the EPR to PAR, together with the Easter and Juan Fernandez microplates, displays a loose pattern facilitating north and south differential motion of the Pacific plate (Fig. 1). Second, several studies indicate that mantle convection may trigger this divergence. Near the surface, a line structure of minimum azimuthal anisotropy (Montagner, 2002) coincides with our shearing channel, and is interpreted as the birth of secondary convection at the base of the lithosphere, also indicative of a future plate reorganization. Deeper seismic tomography (Montelli et al., 2006) of the uppermost thousand kilometers of the Earth, indicate high velocity anomalies in an east–west

elongated area of the central Pacific, similar to our results. Numerical models in which plates are coupled to the underlying mantle (Quéré and Forte, 2006) also show a CMB hotline in the lower mantle, sub-parallel to our zone of weakness. Quéré and Forte (2006) also found another hotline associated with the African rifting, which led them to conclude that the opening of the Nubia–Somalia boundary is related to the mechanical coupling of plates with the convective mantle, without requiring a plume. With other arguments, our numerical study leads to a similar conclusion for the Pacific plate. Finally, lithospheric stress models generated from global mantle circulation and inferred from seismic tomography (Steinberger et al., 2001) indicate a circular tensile region (about half the amplitude of that of our models) centered on the Central Pacific. Steinberger et al. (2001) also note a good correlation between the world's two important tensile zones, the Pacific and Africa, and the location of intraplate volcanism.

## 7. Conclusion

Strain and stress patterns in our models present characteristics that are similar to the few global data available on the area. The Pacific plate is presently in a shear process between the Kermadec Tonga trench and the Easter microplate. This area is becoming a zone of weakness at plate scale where intraplate volcanism expresses itself in response to shearing stresses. Central Pacific volcanism corresponds to break-up spots of shallow origin. This is the first step of a process that could evolve to an opening which will be completed within a few tens of million years. Following Anderson (2001) who proposed that plates are a self-organized system that organizes upper mantle convection, we believe that plate geometry and kinematics are the key to understand plate tectonic evolution at an intermediate time scale. Our hypothesis allows to fill the gap between large scale plate tectonics driven by mantle convection ( $\geq 100$  Myr) and rapid changes in plate motion ( $\leq 5$  Myr), and explain an important part of superficial intraplate volcanism. Improvement of geophysical data is yet needed to confirm the time-scale of this process, whereas full 3D models, accounting for subduction zones and variations in lithospheric thickness, should better reproduce the stress and strain patterns that we simplistically modeled in 2D here.

## Acknowledgments

The authors thank J.-P. Montagner, A. Bonneville, A. Davaille and B. Pelletier for constructive discussions,

two anonymous reviewers for thoughtful reviews and Mark Falvey for its comments on the English.

## References

- Adam, C., Bonneville, A., 2005. The extent of the South Pacific Superswell. *J. Geophys. Res.* 110, B09408. doi:10.1029/2004JB003465.
- Anderson, D., 2001. Plate tectonics as a far-from-equilibrium self-organized system. In: Stein, S., Freymueller, J. (Eds.), *Plate boundary zones*, Geodynamics series, v.30. American Geophysical Union, Washington, D.C., pp. 411–425.
- Anderson, D., 1998. The edges of the mantle. In: Gurnis, M., Wyssession, M., Knittle, E., Buffett, B. (Eds.), *The core–mantle boundary region*, Geophys. Monogr. Ser., vol. 28. American Geophysical Union, pp. 255–271.
- Anderson-Fontana, S., Engeln, J., Lundgren, P., Larson, R., Stein, S., 1986. Tectonics and evolution of the Juan Fernandez Microplate at the Pacific–Nazca–Antarctic triple junction. *J. Geophys. Res.* 91, 2005–2018.
- Atwater, T., 1989. Tectonic maps of the northeast Pacific. In: Winterer, E., Hussong, D., Decker, R. (Eds.), *The Eastern Pacific Ocean and Hawaii*, Vol. N of The Decade of North American Geology Project. The Geological Society of America, pp. 15–72.
- Beavan, J., Tregoning, P., Bevis, M., Kato, T., Meertens, C., 2002. Motion and rigidity of the Pacific Plate and implications for plate boundary deformation. *J. Geophys. Res.* 107, 2261. doi:10.1029/2001JB000282.
- Bercovici, D., 1998. Generation of plate tectonics from lithosphere–mantle flow and void-volatile self-lubrication. *Earth Planet. Sci. Lett.* 154, 139–151.
- Bercovici, D., Ricard, Y., Richards, M., 2000. The relation between mantle dynamics and plate tectonics: A primer. In: Richards, M., Gordon, R., van der Hilst, R. (Eds.), *The history and dynamics of global plate motion*, Geophys. Monogr., vol. 121. American Geophysical Union, Washington, DC, pp. 5–46.
- Bonneville, A., Dosso, L., Hildenbrand, A., 2006. Temporal evolution and geochemical variability of the south Pacific superplume activity. *Earth Planet. Sci. Lett.* 244, 251–269. doi:10.1016/j.epsl.2005.12.037.
- Brace, W., Kohlstedt, D., 1980. Limits on lithospheric stress imposed by laboratory experiments. *J. Geophys. Res.* 85, 6248–6252.
- Burov, E., Poliakov, A., 2001. Erosion and rheology controls on syn- and post-rift evolution: verifying old and new ideas using a fully coupled numerical model. *J. Geophys. Res.* 106, 16461–16481.
- Chamot-Rooke, N., LePichon, X., 1989. Zensu Ridge mechanical model of formation. *Tectonophysics* 160, 175–193.
- Clouard, V., Bonneville, A., 2005. Ages of seamounts, islands and plateaus on the Pacific Plate. In: Foulger, G., Natland, J., Presnall, D., Anderson, D. (Eds.), *Plates, plumes and paradigms*, Special Paper 388. Geological Society of America, Boulder, CO, pp. 71–90.
- Clouard, V., Bonneville, A., 2001. How many Pacific hotspots are fed by deep-mantle plumes? *Geology* 29, 695–698.
- Courtillot, V., Davaille, A., Besse, J., Stock, J., 2003. Three distinct types of hotspots in the Earth's mantle. *Earth Planet. Sci. Lett.* 205, 295–308.
- Cundall, P., Board, M., 1988. A microcomputer program for modeling large-strain plasticity problems. *Numer. Methods Geomech.* 6, 2101–2108.
- Davaille, A., 1999. Simultaneous generation of hotspots and super-swells by convection in a heterogeneous planetary mantle. *Nature* 402, 756–760.
- Davaille, A., Stutzmann, E., Silveira, G., Besse, J., Courtillot, V., 2005. Convective patterns under the indo-atlantic “box”. *Earth Planet. Sci. Lett.* 239, 233–252.

- DeMets, C., Gordon, R., Argus, D., Stein, S., 1990. Current plate motions. *Geophys. J. Int.* 101, 425–478.
- DeMets, C., Gordon, R., Argus, D., Stein, S., 1994. Effects of recent revisions to the magnetic reversal time scale on estimates of current plate motions. *Geophys. Res. Lett.* 21 (20), 2191–2194.
- Deplus, C., Diament, M., Hebert, H., Bertrand, G., Dominguez, S., Dubois, J., Patriat, J.M.J.P., Pontoise, B., Sibilla, J.J., 1998. Direct evidence of active deformation in the eastern Indian oceanic plate. *Geology* 26, 131–134.
- Dunbar, J., Sandwell, D.T., 1988. A boudinage model for crossgrain lineations. *EOS. Trans. AGU*, 69, 1429.
- England, P., McKenzie, D., 1983. Correction to: a thin viscous sheet model for continental deformation. *Geophys. J. R. Astr. Soc.* 73, 523–532.
- Escartin, J., Cowie, P., Searle, R., Allerton, S., Mitchell, N., Macleod, C., Slootweg, A., 1999. Quantifying tectonic strain and magmatic accretion at a slow spreading ridge segment, Mid-Atlantic Ridge, 29°N. *J. Geophys. Res.* 104, 10421–10437.
- Faccenna, C., Heuret, A., Funicello, F., Lallemand, S., Becker, T., 2007. Predicting trench and plate motion from the dynamics of a strong slab. *Earth Planet. Sci. Lett.* 257, 29–36. doi:10.1016/j.epsl.2007.02.016.
- Gerbault, M., 2000. At what stress level is the Central Indian Ocean lithosphere buckling? *Earth Planet. Sci. Lett.* 178, 165–181.
- Gerbault, M., Henrys, S., Davey, F., 2003. Numerical models of lithospheric deformation forming the Southern Alps of New Zealand. *J. Geophys. Res.* 108 (B7), 2341. doi:10.1029/2002JB001880.
- Gerbault, M., Poliakov, A., Daignieres, M., 1998. Prediction of faulting from the theories of elasticity and plasticity: what are the limits? *J. Struct. Geol.* 20, 301–320.
- Gill, J., Gorton, M., 1973. A proposed geological and geochemical history of eastern Melanesia. In: Coleman, P. (Ed.), *The Western Pacific: Island Arc, Marginal Seas, Geochemistry*. University of Western Australia Press, Perth, pp. 543–566.
- Grand, S., van der Hilst, R., Widiyantoro, S., 1997. Global seismic tomography: a snapshot of convection in the Earth. *GSA Today* 7, 1–7.
- Hamburger, M., Isacks, B., 1987. Deep earthquakes in the Southwest Pacific: a tectonic interpretation. *J. Geophys. Res.* 92, 13841–13854.
- Heuret, A., Lallemand, S., 2005. Plate motions, slab dynamics and back-arc deformation. *Phys. Earth Planet. Inter.* 149, 31–51.
- Hill, R., 1950. *Mathematical Theory of Plasticity*, Engineering Science Series 11. Oxford University Press, Oxford.
- Hirano, N., Takahashi, E., Yamamoto, J., Abe, N., Ingle, S.P., Kaneoka, T.H.I., Kimura, J.I., Ishii, T., Ogawa, Y., Machida, S., Suyehiro, K., 2006. Volcanism in response to plate flexure. *Science* 313, 1426–1428. doi:10.1126/science.1128235.
- Hobbs, B., Ord, A., 1989. Numerical simulations of shear band formation in a frictional-dilatant material. *Ingenieur-Archiv* 59, 209–220.
- Ito, G., McNutt, M., Gibson, R.L., 1995. Crustal structure of the Tuamotu Plateau, 15° S, implications for its origin. *J. Geophys. Res.* 100, 8097–8114.
- Kachanov, L., 1974. *Fundamentals of the theory of plasticity*. Mir, Moscow.
- Keir, D., Ebinger, C.J., Stuart, G.W., Daly, E., Ayele, A., 2006. Strain accommodation by magmatism and faulting as rifting proceeds to breakup: seismicity of the northern Ethiopian rift. *J. Geophys. Res.* 111, B05314. doi:10.1029/2005JB003748.
- Khazaradze, G., Klotz, J., 2003. Short-and long-term effects of GPS measured crustal deformation rates along the south central Andes. *J. Geophys. Res.* 108, 2289. doi:10.1029/2002JB001879.
- Kohlstedt, D., Evans, B., Mackwell, S., 1995. Strength of the lithospheric: constraints imposed by laboratory experiments. *J. Geophys. Res.* 100, 17587–17602.
- Koppers, A.A.P., Staudigel, H., Pringle, M.S., Wijbrans, J.R., 2003. Short-lived and discontinuous intraplate volcanism in the South Pacific: hot spots or extensional volcanism? *Geochem. Geophys. Geosyst.* 4 (10), 1089. doi:10.1029/2003GC000533.
- Kroenke, L.W., Walker, D.A., 1986. Evidence for the formation of a new trench in the western Pacific. *Eos Trans. AGU* 67, 145–146.
- Kroenke, L., Wessel, P., Sterling, N., 2002. Initiation of subduction, forced changes in absolute plate motion and the development of rifting: A Pacific perspective. *Fall Meet. Suppl.*, Vol. 83, pp. OS11E–OS71E.
- Lavier, L., Buck, W., Poliakov, A., 1999. Self-consistent rolling-hinge model for the evolution of large-onset low-angle normal faults. *Geology* 27, 1127–1130.
- Leffler, X., Stein, S., Mao, A., Dixon, T., Ellis, M., Ocala, L., Sacks, I., 1997. Constraints on present-day shortening rate across the Central Eastern Andes from GPS measurements. *Geophys. Res. Lett.* 24, 1031–1034.
- Lithgow-Bertelloni, C., Richards, M., 1998. Dynamics of cenozoic and mesozoic plate motions. *Rev. Geophys.* 36, 27–28.
- Mayes, C., Lawver, L., Sandwell, D., 1990. Tectonic history and new isochron chart of the South Pacific. *J. Geophys. Res.* 95, 8543–8567.
- McHone, J.G., 2000. Non-plume magmatism and rifting during the opening of the central Atlantic Ocean. *Tectonophysics* 316, 287–296.
- McNutt, M., 1998. Superswell. *Rev. Geophys.* 36, 211–244.
- McNutt, M., Fisher, K., 1987. The South Pacific Superswell. In: Keating, B., Fryer, P., Batiza, R., Boehlert, G. (Eds.), *Seamounts, Islands, and Atolls*, *Geophys. Monogr. Ser.*, vol. 43. American Geophysical Union, Washington, DC, pp. 25–34.
- Montagner, J., 2002. Upper mantle low anisotropy channels below the Pacific Plate. *Earth Planet. Sci. Lett.* 202, 263–274.
- Montelli, R., Nolet, G., Dahlen, F., Masters, G., 2006. A catalogue of deep mantle plumes: new results from finite-frequency tomography. *Geochem. Geophys. Geosyst.* 7, Q11007. doi:10.1029/2006GC001248.
- Morgan, W., 1971. Convection plumes in the lower mantle. *Nature* 230, 42–43.
- Morgan, W., 1972. Plate motions and deep mantle convection. *Geol. Soc. Am. Mem.* 132, 7–22.
- Morgan, W., 1978. Rodriguez, Darwin, Amsterdam...a second type of hotspot island. *J. Geophys. Res.* 83, 5355–5360.
- Naar, D., Hey, R., 1991. Tectonic evolution of Easter Microplate. *J. Geophys. Res.* 96, 7961–7993.
- Odé, H., 1960. Faulting as a velocity discontinuity in plastic deformation. *Mem. Geol. Soc. Am.* 79, 293–321.
- Pelletier, B., Calmant, S., Pillet, R., 1998. Current tectonics of the tonga-new hebrides region. *Earth Planet. Sci. Lett.* 164, 263–276.
- Poliakov, A., Podladchikov, Y., 1992. Diapirism and topography. *Geophys. J. Int.* 109, 553–564.
- Prawirodirdjo, L., Bock, Y., 2004. Instantaneous global plate motion model from 12 years of continuous gps observations. *J. Geophys. Res.* 109, B08405. doi:10.1029/2003JB002944.
- Provost, A.S., Chery, J., Hassani, R., 2003. 3d mechanical modeling of the gps velocity field along the north anatolian fault. *Earth Planet. Sci. Lett.* 209, 361–377.
- Pysklywec, R., Mitrovica, J., Ishii, M., 2003. Mantle avalanche as a driving force for tectonic reorganization in the southwest Pacific. *Earth Planet. Sci. Lett.* 209, 29–38.
- Quére, S., Forte, A., 2006. Influence of past and present-day plate motions on spherical models of mantle convection: implications

- for mantle plumes and hotspots. *Geophys. J. Int.* 165, 1041–1057. doi:10.1111/j.1365-246X.2006.02990.x.
- Ranalli, G., 1995. *Rheology of the Earth*. Chapman and Hall, London.
- Regenauer-Lieb, K., 1999. Dilatant plasticity applied to Alpine collision: ductile void growth in the intraplate area beneath the Eifel Volcanic Field. *J. Geodyn.* 27, 1–21.
- Regenauer-Lieb, K., Petit, J., 1997. Cutting of the European continental lithosphere: plasticity theory applied to the present Alpine collision. *J. Geophys. Res.* 102, 7731–7746.
- Richards, M., Duncan, R., Courtillot, V., 1989. Flood basalts and hot-spot tracks: plume heads and tails. *Science* 246, 103–107.
- Richards, M., Gordon, R., van der Hilst, R., 2000. Introduction: plate tectonics and mantle convection three decades later. In: Richards, M., Gordon, R., van der Hilst, R. (Eds.), *The history and dynamics of global plate motion*, *Geophys. Monogr.*, vol. 121. American Geophysical Union, Washington, DC, pp. 1–4.
- Sandwell, D., Fialko, Y., 2004. Warping and cracking of the Pacific plate by thermal contraction. *J. Geophys. Res.* 109, B10411. doi:10.1029/2004JB003091.
- Sella, G., Dixon, T., Mao, A., 2002. Revel: A model for recent plate velocities from space geodesy. *J. Geophys. Res.* 107, 2081. doi:10.1029/2000JB000033.
- Shemenda, A., 1992. Horizontal lithosphere compression and subduction: constraints provided by physical modeling. *J. Geophys. Res.* 97, 11097–11116.
- Sheth, H., 1999. A historical approach to continental flood basalt volcanism: insights into pre-volcanic rifting, sedimentation, and early alkaline. *Earth Planet. Sci. Lett.* 168, 19–26.
- Steinberger, B., Schmelting, H., Marquart, G., 2001. Large-scale lithospheric stress field and topography induced by global mantle circulation. *Earth Planet. Sci. Lett.* 186, 75–91.
- Tackley, P., 2000. The quest for self-consistent generation of plate tectonics in mantle convection models. In: Richards, M., Gordon, R., van der Hilst, R. (Eds.), *The history and dynamics of global plate motion*, *Geophys. Monogr.* 121. American Geophysical Union, Washington, DC, pp. 47–72.
- Tapponnier, P., Molnar, P., 1976. Slip line field theory and large scale continental tectonics. *Nature* 264, 319–324.
- van der Hilst, R., Widiyantoro, S., Engdahl, E., 1997. Evidence for deep mantle circulation from global tomography. *Nature* 386, 578–584.
- Weissel, J.K., Anderson, R.N., Geller, C.A., 1980. Deformation of the Indo-Australian plate. *Nature* 287, 284–291.
- Wessel, P., Kroenke, L.W., 2007. Reconciling late Neogene Pacific absolute and relative plate motion changes. *Geochem. Geophys. Geosyst.* 8 (8), 8001. doi:10.1029/2007GC001636.
- Wilson, J.T., 1973. Mantle plumes and plate motions. *Tectonophysics* 19, 149–164.
- Yang, Y., Liu, M., 2002. Deformation of convergent plates: evidence from discrepancies between GPS velocities and rigid-plate motions. *Geophys. Res. Lett.* 29. doi:10.1029/2001GL013391.
- Zhong, S., Ritzwoller, M., Shapiro, N., Landuyt, W., Huang, J., Wessel, P., 2007. Bathymetry of the Pacific plate and its implications for thermal evolution of lithosphere and mantle dynamics. *J. Geophys. Res.* 112, B06412. doi:10.1029/2006JB004628.